

## Supporting Information

### Physical cross-linked hydrogel derived smart windows: anti-freezing and fast thermal responsive performance

Gang Li<sup>†</sup>, Jiwei Chen<sup>†</sup>, Zhaonan Yan, Shancheng Wang, Yujie Ke, Wei Luo, Huiru Ma, Jianguo Guan\*, Yi Long\*

### Supporting Figures

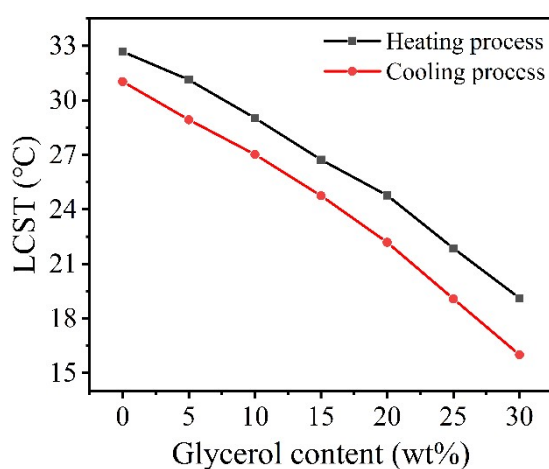


Figure S1. LCST as a function of glycerol content.

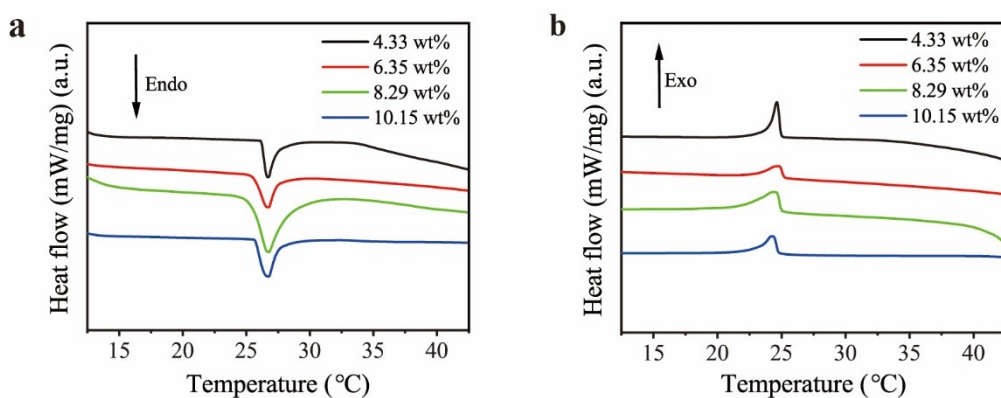


Figure S2. DSC analysis for the LCST of noncovalent crosslinked viscous PNIPAM GW solutions prepared with different concentration of NIPAM: (a) heating stage and (b) cooling stage.

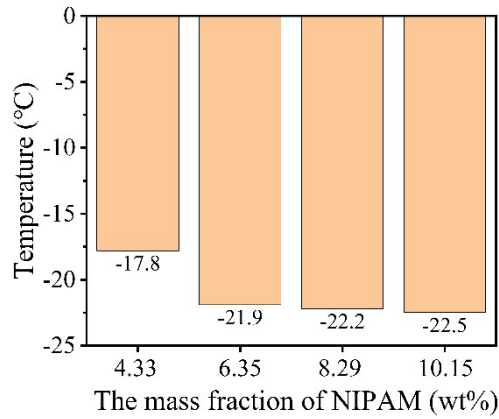


Figure S3. DSC curves of freezing point, noncovalent crosslinked viscous PNIPAM GW solutions prepared different concentration of NIPAM.

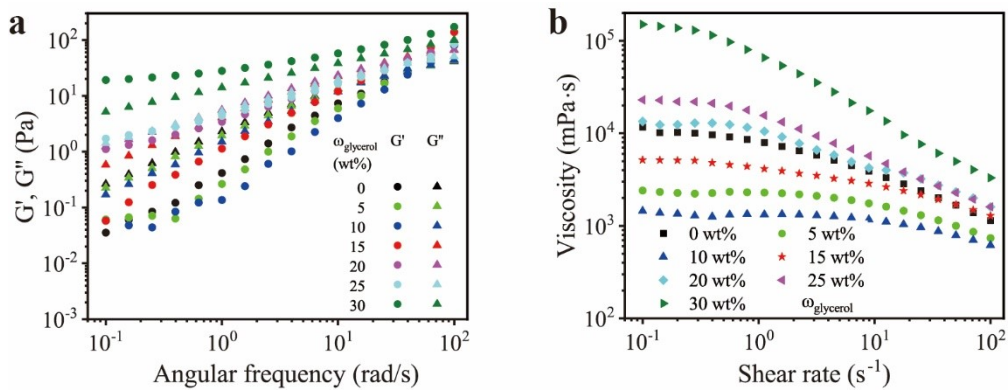


Figure S4. (a) The storage modulus ( $G'$ ) and loss modulus ( $G''$ ) as the function of angular frequency for glycerol of varying content. (b) Viscosity as a function of shear rate for glycerol of varying content.

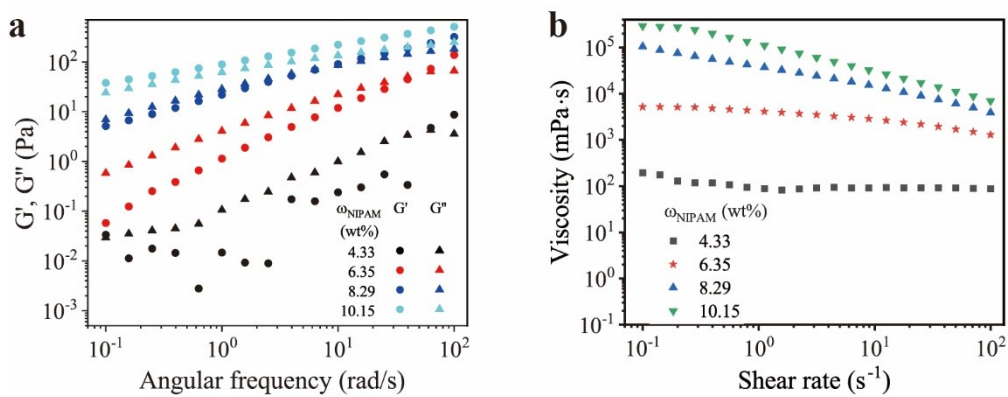


Figure S5. (a) The storage modulus ( $G'$ ) and loss modulus ( $G''$ ) as the function of angular frequency for NIPAM of varying content. (b) Viscosity as a function of shear rate for NIPAM of varying content.

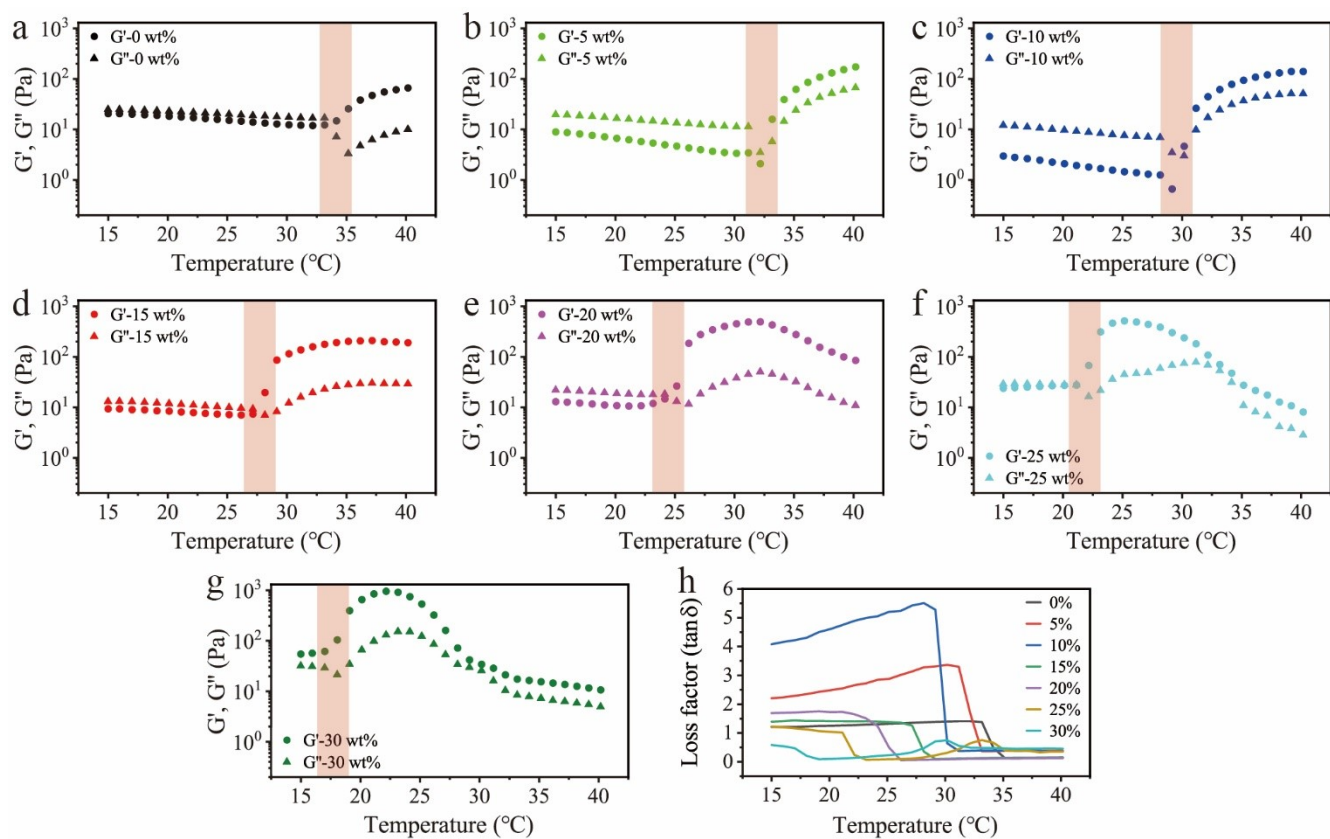


Figure S6. (a-g) The storage modulus ( $G'$ ) and loss modulus ( $G''$ ) as the function of temperature for glycerol of varying content. (h) Loss factor as the function of temperature for glycerol of varying content.

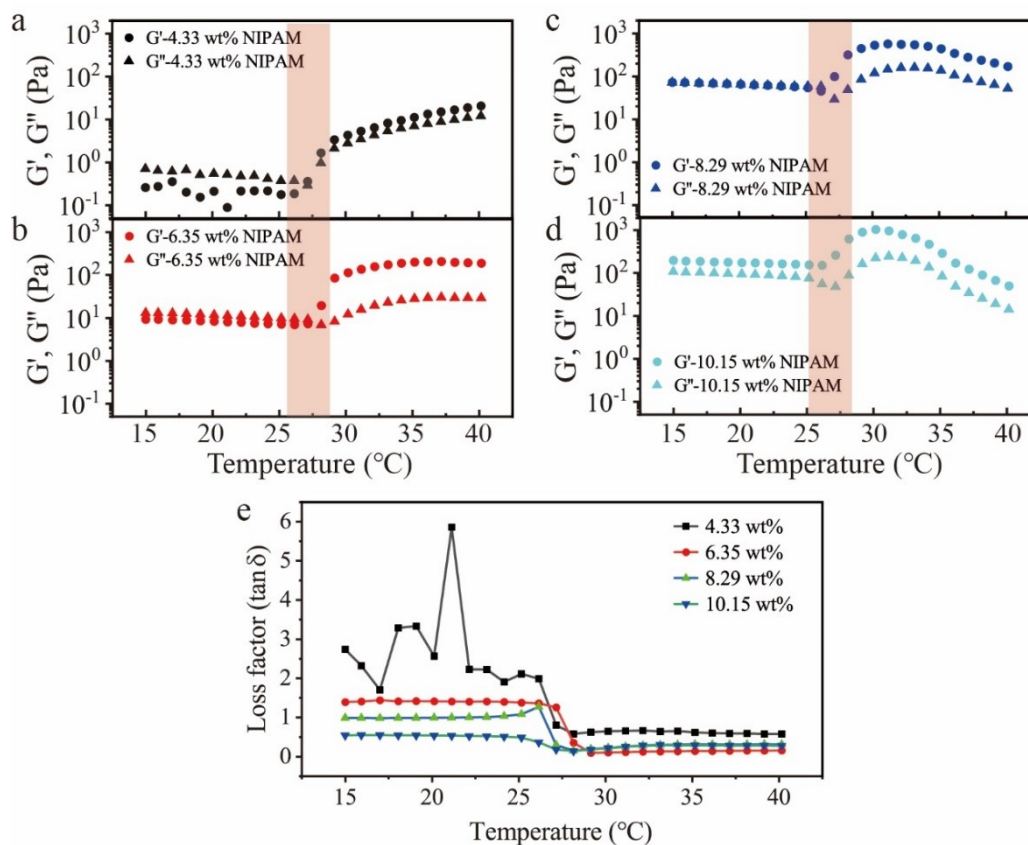


Figure S7. (a-d) The storage modulus ( $G'$ ) and loss modulus ( $G''$ ) as the function of temperature for NIPAM of varying content. (e) Loss factor as the function of temperature for NIPAM of varying content.

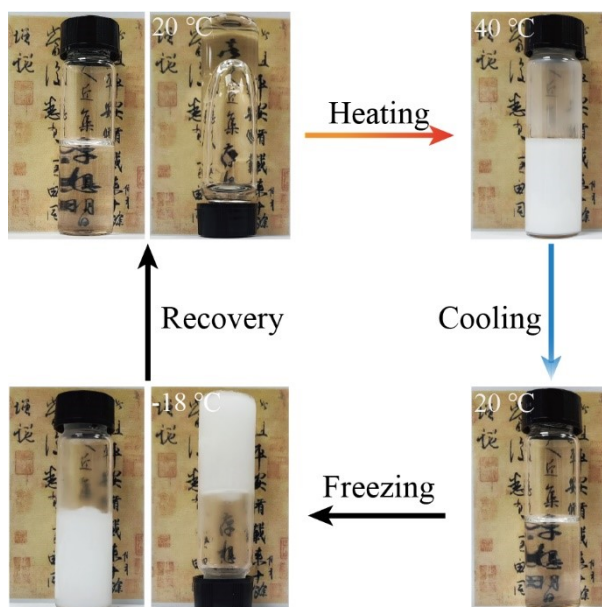


Figure S8. The photos of the noncovalent crosslinked PNIPAM solutions prepared with water after heating, cooling, and freezing

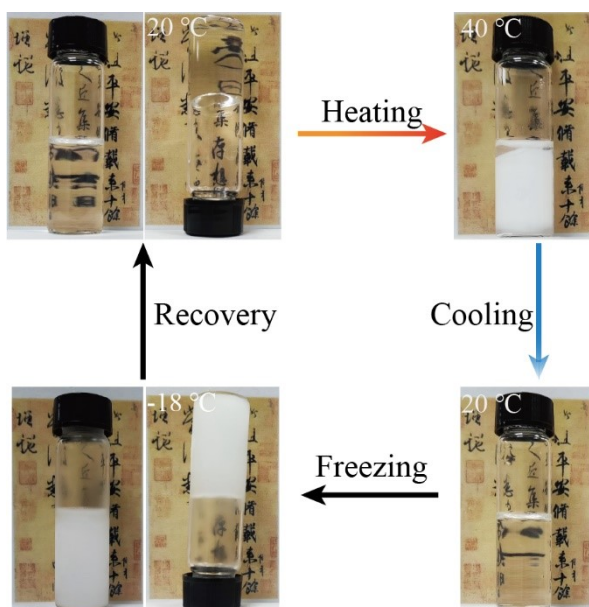


Figure S9. The photos of the covalent crosslinked PNIPAM hydrogel prepared with water after heating, cooling, and freezing.

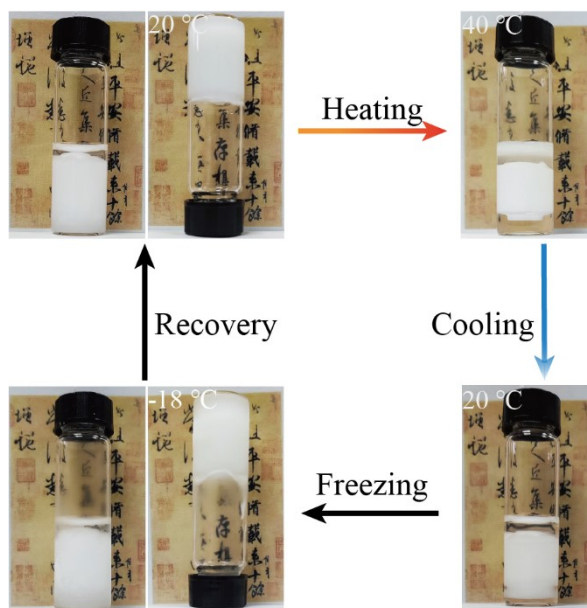


Figure S10. The photos of the covalent crosslinked PNIPAM GW hydrogel prepared with 15 wt% glycerol of total solvent after heating, cooling, and freezing.



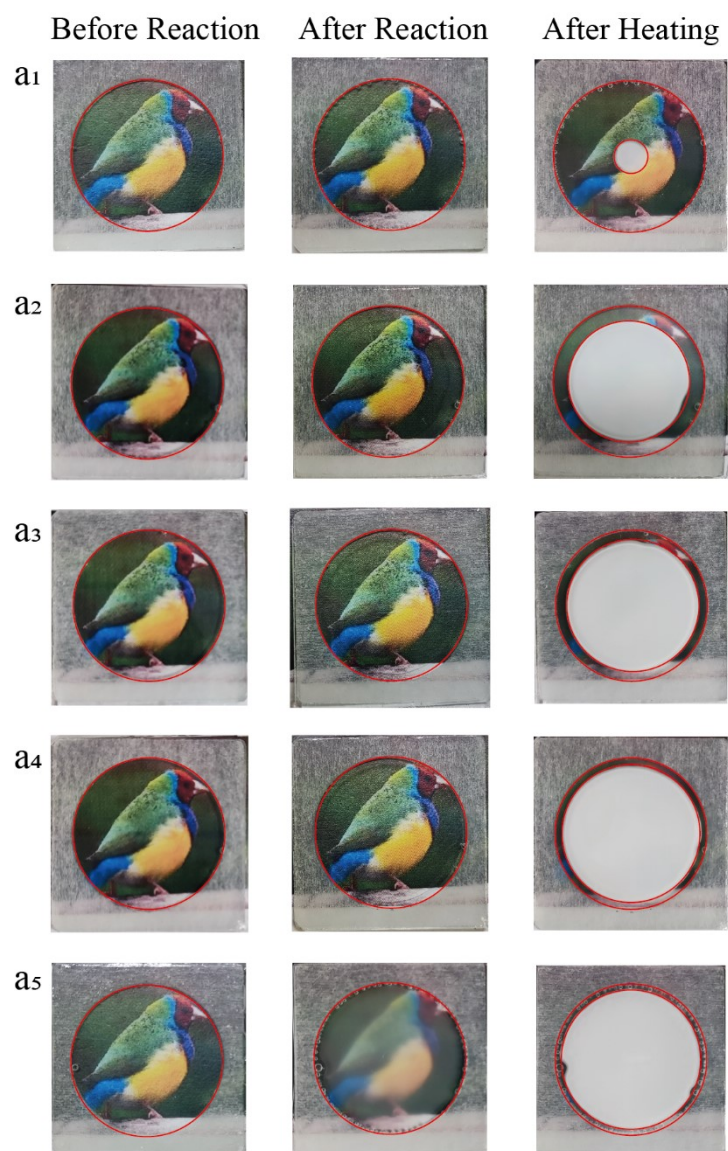


Figure S11. Photographs of smart windows based on the covalent crosslinked PNIPAM hydrogels in different states via the in-situ polymerization with different NIPAM mass fraction. (a<sub>1</sub>) 4.33 wt%, (a<sub>2</sub>) 8.29 wt%, (a<sub>3</sub>) 10.15 wt%, (a<sub>4</sub>) 11.93 wt%, (a<sub>5</sub>) 14.48 wt%.

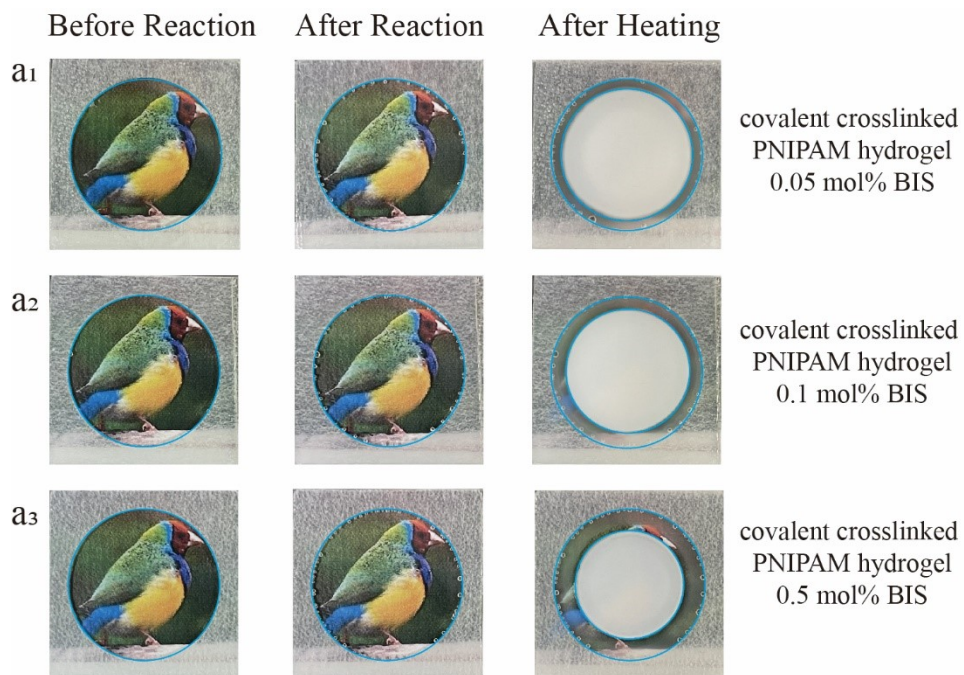


Figure S12. Photographs of smart windows based on the covalent crosslinked PNIPAM hydrogels in different states via the in-situ polymerization with different BIS concentration. (a<sub>1</sub>) 0.05 mol%, (a<sub>2</sub>) 0.1 mol%, (a<sub>3</sub>) 0.5 mol%.

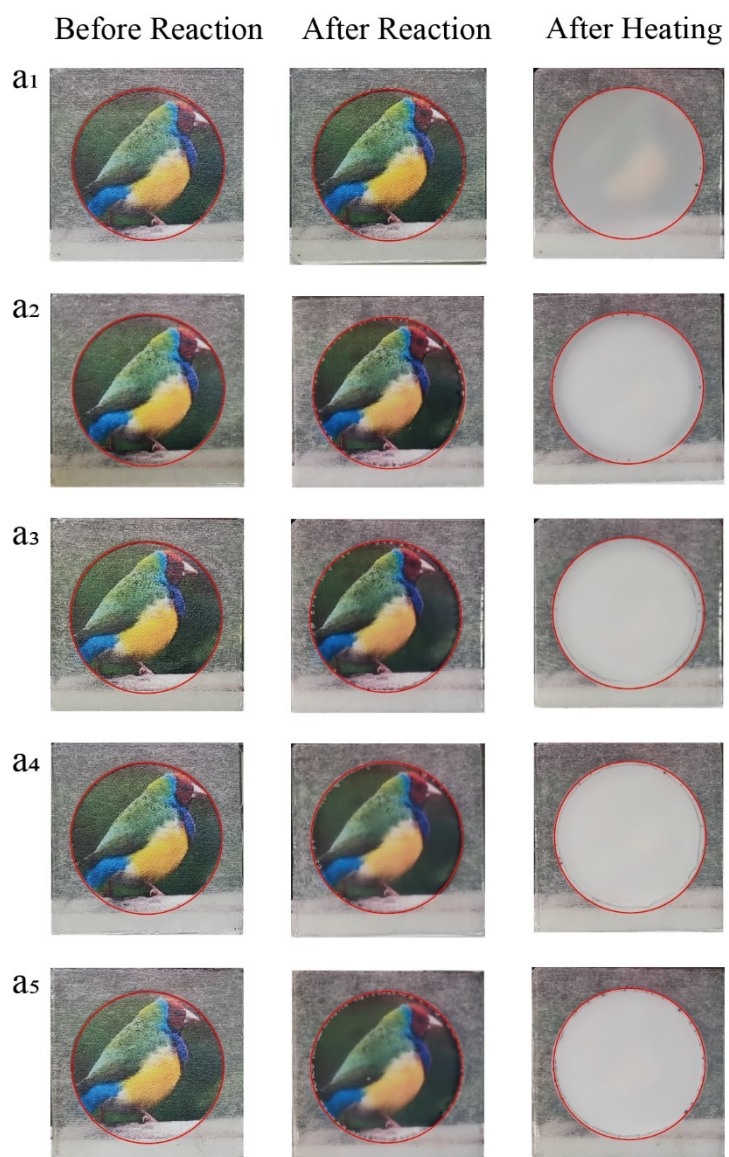


Figure S13. Photographs of smart windows based on the noncovalent crosslinked viscous PNIPAM GW solutions in different states via the in-situ polymerization with different NIPAM mass fraction. (a<sub>1</sub>) 4.33 wt%, (a<sub>2</sub>) 8.29 wt%, (a<sub>3</sub>) 10.15 wt%, (a<sub>4</sub>) 11.93 wt%, (a<sub>5</sub>) 14.48 wt%.



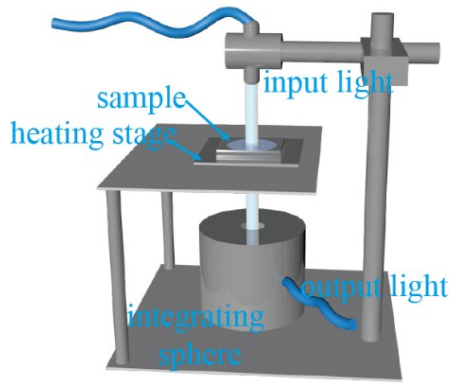


Figure S14. Diagram of the thermal response performance measurement system

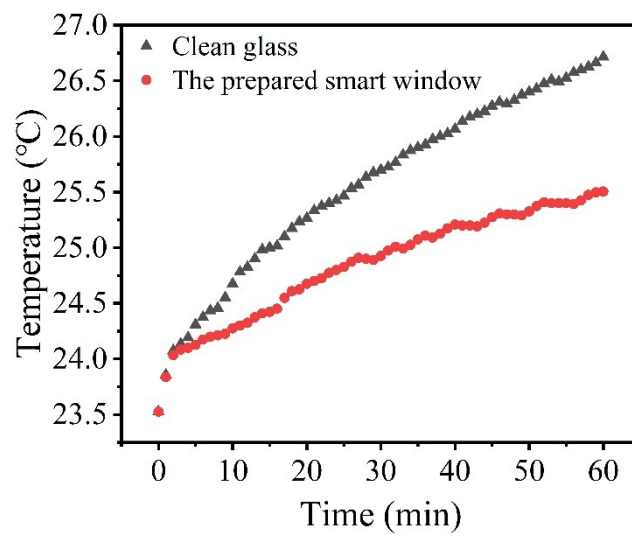


Figure S15. Energy-saving demonstration results of the experimental air temperature reading.

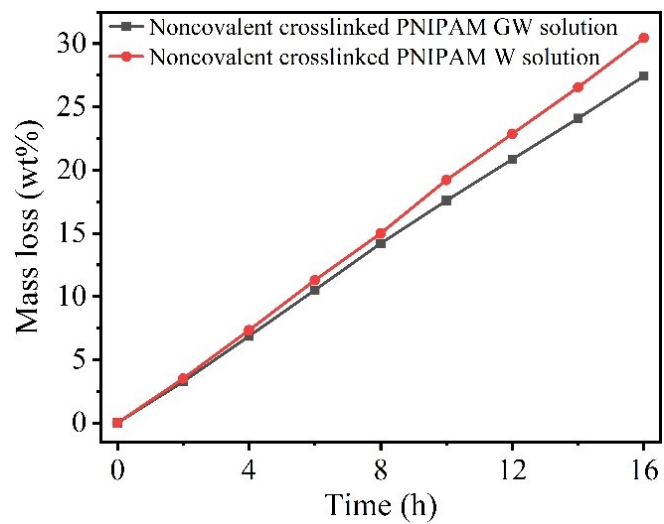


Figure S16. Evaporation curves at 80°C

## Supporting Table

Table S1. Interaction energy between PNIPAM, water, and glycerol

Model	Interaction energy (Kcal/mol)
W-W	-3.45
G-G	-3.09
G-W	-4.97
G-PNIPAM	-6.91
W-PNIPAM	-13.63
G-W-PNIPAM	-19.49

## Supporting Videos

**Video S1.** The phase transition video of the smart window triggered by finger touch.